Applied Biochemistry and Biotechnology
https://doi.org/10.1007/s12010-021-03531-x

ORIGINAL ARTICLE

Paper-Based Enzymatic Colorimetric Assay for Rapid Malathion Detection

Jian-Hui Li[1] · Xue-Lei Deng[2] · Yu-Lian Zhao[2] · Xiao-Yan Zhang[2] · Yun-Peng Bai[2]

Received: 13 September 2020 / Accepted: 23 February 2021/Published online: 30 March 2021

Abstract

Due to their unique properties, paper-based biosensors have attracted attention as inexpensive devices for on-site analysis. To achieve fast and sensitive detection of analytes, immobilization of enzymes with high apparent activities on paper is highly desirable; however, this is challenging. Herein, we report an improved approach to attach a malathion degrading enzyme, *Po*OPH$_{M9}$, on paper via an interlocking network of Pluronic F127 (PF127)–poly(acrylic acid)–enzyme conjugates. The addition of PF127 improved retention of enzymatic activity as the apparent kinetic constant V_{max} of the immobilized enzyme increased two-fold compared with the paper prepared without PF127. The PF127–poly(acrylic acid)–*Po*OPH$_{M9}$ papers provided rapid colorimetric detection of malathion at 0.1–50 mM. The detection was completed within 5 min using a smartphone and image analysis software. As a proof-of-concept, malathion-contaminated water, plant, and apple samples were analyzed with the papers successfully. This material is promising for on-site rapid analysis of malathion-contaminated samples.

Keywords Enzyme immobilization · Paper-based biosensor · Malathion detection · Polymer–enzyme conjugate · Organophosphate hydrolase

Introduction

Organophosphorus pesticides are widely used in modern agriculture as insecticides and fungicides because they are highly efficient, broad spectrum, and persistent [1]. Malathion

Jian-Hui Li and Xue-Lei Deng contribute equally to this work.

✉ Xiao-Yan Zhang
xyzhang@ecust.edu.cn

✉ Yun-Peng Bai
ybai@ecust.edu.cn

[1] College of Marine Life Sciences, Ocean University of China, Qingdao 266003, China

[2] State Key Laboratory of Bioreactor Engineering, East China University of Science and Technology, 130 Meilong Road, Shanghai 200237, China

was first registered as an insecticide in the 1950s and, according to the US Environmental Protection Agency, it has been among the best-selling generic organophosphate insecticides worldwide since the 1980s [2]. Large quantities of organophosphorus pesticide residues in the environment are a threat to public health and safety [3–5]. Rapid detection of organophosphorus residues in the environment and on food is highly desirable for public health reasons. Currently, several methods are used for the determination of organophosphorus pesticides, including gas chromatography [6], high-performance liquid chromatography [7], and capillary electrophoresis [8]. These methods require commercial instruments and are rather complicated, expensive, and time-consuming, which means they are inappropriate for field applications and rapid real-time detection and analysis [9].

To avoid the above problems, paper-based enzyme biosensors have been developed that are cost-effective, easy to use, and provide rapid detection of pesticides with minimal equipment requirements [10–15]. Paper is promising as a substrate for enzyme immobilization because it is biodegradable, biocompatible, hydrophilic, and inexpensive [16]. Enzymes can be trapped in cellulose by covalent binding [17], physical adsorption [18, 19], and deposition [20–22]. Covalent binding to the functionalized surface of cellulose generally results in a decrease in catalytic activity due to conformational change of the enzyme. Physical adsorption and deposition can retain enzymatic activity, but enzymes are easily lost during application. Recently, Riccardi et al. developed a novel interlocking method for trapping enzymes on paper for glucose detection [23], and later, several colorimetric assays for detection of various targets were developed by other groups [24–26]. In this method, an enzyme was first cross-linked to poly(acrylic acid) (PAA) to form an enzyme–polymer conjugate, which could be interlocked with cellulose fibers and trapped in paper voids. The whole assay takes 15–45 min for colorimetric detection of glucose, which is still not fast enough for on-site analysis [23].

Previously, we developed a high-yield fermentation method to produce an efficient malathion hydrolase, *Po*OPH$_{M9}$, which was engineered from a wild-type lactonase OPHC2 by directed evolution and can break down the P-S bond in malathion [27, 28]. Later, we presented a new method to prepare polymer–enzyme conjugates with Pluronic F127 (PF127) that showed high thermostability and worked over a broad pH range [29]. PF127 conjugated with *Po*OPH$_{M9}$ by surface interaction instead of covalent bonding, and enhanced the activity of *Po*OPH$_{M9}$ 2.5-fold. Inspired by this result, in the present study, we aimed to prepare a new bio-ink containing PF127, PAA, and *Po*OPH$_{M9}$. We hypothesized that PF127 would improve the retention of *Po*OPH$_{M9}$ activity during covalent bonding with PAA. The polymer–enzyme conjugates were then trapped in paper to prepare PAA–PF127–*Po*OPH$_{M9}$ papers (Scheme 1). The hydrolyzed product, mercaptan, reacted with Ellman's reagent, 5,5′-dithiobis(2-nitrobenzoic acid) (DNTB), to produce a bright or dark yellow color for colorimetric detection. We aimed to use this new paper for the fast, on-site detection of malathion residues in the environment.

Materials and Methods

Chemicals and Reagents

All chemicals were purchased from Sangon Biotech (Shanghai, China), Sigma-Aldrich (St. Louis, MO), and Lingfeng Chemical (Shanghai, China), and used without further treatment unless otherwise indicated. Analytical grade methanol, glycerol, and ethyl acetate were

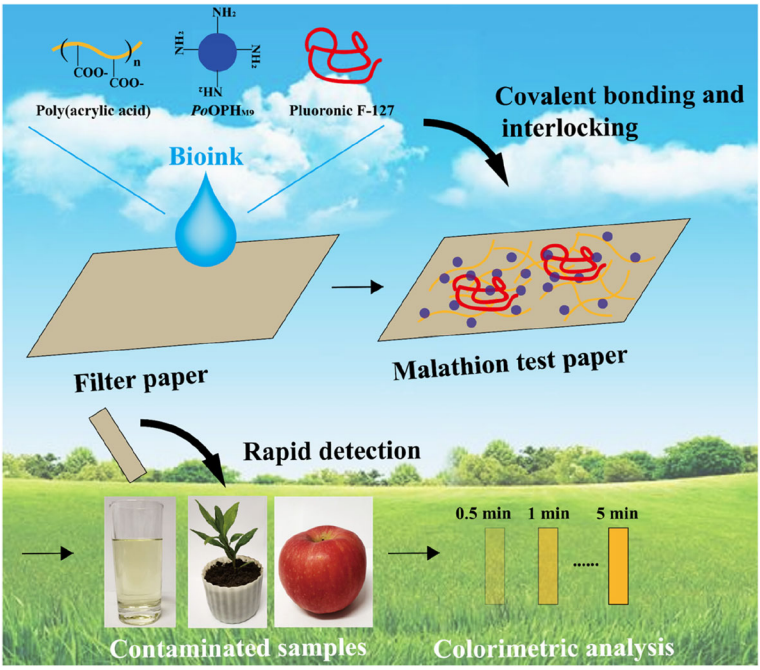

Scheme 1 Illustration of the preparation and application of malathion test papers

purchased from Macklin Biochemical (Shanghai, China). Malathion, methyl parathion, dimethoate, carbaryl, and DDT were purchased from the Shanghai Pesticide Research Institute. Filter paper was purchased from Hangzhou Special Industry (Hangzhou, China). *Pichia pastoris* strain X33/pPICZαA-Δpoophm9 was prepared and stored in our laboratory.

Enzyme Expression and Treatment

The *P. pastoris* strain X33/pPICZαA-Δpoophm9 was used to express enzymes via a three-step fermentation, and enzyme expression was induced by the addition of methanol [28]. After 18–24 h, glycerol was depleted and the dissolved oxygen level increased rapidly up to 100% when the optical density at 600 nm reached approximately 200. Aliquots of the supernatant were taken at fixed intervals to measure the enzyme titer of the culture broth. The fermentation was terminated when the enzyme production stopped increasing. After fermentation, the supernatant was centrifuged at 15,500*g* for 20 min and then filtered through a 0.22-μm membrane to remove cell debris. The enzyme solution was further concentrated to 150 mL with a 10-kDa filter membrane, stored in a freezer at −80 °C for 8 h, and then freeze-dried for 24 h to yield *Po*OPH$_{M9}$ enzyme powder.

Fabrication of Paper-Based Biosensors

To fabricate PAA–*Po*OPH$_{M9}$ papers, an appropriate volume of PAA solution, phosphate buffer (50 mM, pH 7.0) or Tris-HCl buffer (50 mM, pH 9.0), and 1-ethyl-3-(3-dimethylaminopropyl)-carbodiimide (EDC) (50 mM) were stirred together at room temperature for 15 min to activate the PAA. Then, *Po*OPH$_{M9}$ (10 mg/mL) was added. Typically, the

activated mixture (PAA–*Po*OPH$_{M9}$) of 50 μL was immediately transferred to the filter paper and cross-linking proceeded, which interlocked the resulting gel within the paper voids (PAA–*Po*OPH$_{M9}$–cellulose). After cooling at room temperature, the paper was washed with 6 mL deionized (DI) water for 2 h to remove free enzymes, and then dried again for use.

To fabricate the PF127–PAA–*Po*OPH$_{M9}$ biosensor, *Po*OPH$_{M9}$ and PF127 in Tris-HCl buffer (50 mM, pH 9.0) were added together to the PAA solution after EDC activation following the procedure described above. The mixture (PF127–PAA–*Po*OPH$_{M9}$) of 50 μL was immediately transferred to the filter paper for cross-linking and interlocking. Then the paper was washed with 6 mL DI water for 2 h to remove free enzymes and dried before use.

The SDS-PAGE of the polymer-enzyme composite was performed as below. First, 5% concentrated gel and 12.5% separation gel were prepared. The sample solution was added with 10 μL 2% SDS solution containing 10% β-mercaptoethanol. Then, the sample was heated at 95 °C for 15 min and loaded on the gel with 4 μg sample per lane. The electrophoresis was run in the electrophoretic device at 200 V. The gel was dyed with 10% acetic acid, 10% isopropanol and 0.1% Coomassie brilliant blue R250, and decolorized overnight in 10% acetic acid.

Enzymatic Assay with the Paper-Based Biosensor

To determine enzyme loading on the filter paper, the total protein content (P_t) and the protein content in the washing water (P_w) were determined by the Coomassie brilliant blue method. Using the protein content of a blank filter paper in the washing water as the control, the enzyme loading (%) of the paper-based biosensor was calculated as follows:

$$\text{Enzyme loading} = (P_t - P_w)/P_t \times 100\% \tag{1}$$

To determine the apparent activity of *Po*OPH$_{M9}$ on the paper, 20 mg of paper with immobilized enzymes was added to 50 mM Tris-HCl buffer (pH 9.0) containing 2 mM Ellman's reagent (5,5-dithiobis(2-nitrobenzoic acid)). Then, 0.5 mM malathion was added, and the hydrolyzed product of malathion, mercaptan, reacted with Ellman's reagent. This colorimetric reaction caused an increase in the absorbance at 412 nm, which was monitored by a spectrophotometer (DU-730, Beckman) for 1 min. The total enzyme activity was calculated using Eq. 2.

$$U = \frac{D \times 10^3 \times (\Delta A_1 - \Delta A_2) \times V_t}{\varepsilon \times V_S \times d} \tag{2}$$

One unit of enzyme activity (U) was defined as the amount of enzyme that catalyzed the hydrolysis of 1 μmol of malathion per min under the above conditions. In Eq. 2, D is the dilution ratio; ΔA_1 and ΔA_2 are the absorbance changes of the sample and the blank, respectively; V_t is the total volume (mL) of the reaction solution; ε is the molar absorbance (13600 L mol^{-1} cm^{-1}); V_s is the enzyme volume (mL); and d is optical path length (cm) of the cuvette.

The initial rates of the reactions at different substrate concentrations with papers were measured using the initial slopes of the time-course curves of color intensity and the apparent kinetic parameters were calculated by fitting the kinetic curve to the Michaelis–Menten model.

Detection of Malathion by the PF127–PAA–*Po*OPH$_{M9}$ Biosensor

A circle (ø 6 mm) was punched out of the prepared enzymatic filter paper. Ellman's reagent (5 μL) and malathion (5 μL, 0.1–30 mM) were dissolved in 50 mM Tris-HCl buffer (pH 9.0) and

added to the paper. The hydrolyzed product of malathion reacted with Ellman's reagent for 0–60 min. After adding malathion, color images were taken using an auto-focusing smartphone that was fixed 10 cm above the paper. The images were analyzed using ImageJ, and color intensities were calculated from gray values as follows:

$$\text{Color intensity} = 255 - \text{gray values} \tag{3}$$

Here, 255 corresponds to the grayscale of white and 0 corresponds to the gray scale of black. Thus, a higher color intensity calculated according to Eq. 3 corresponds to a darker color observed on the enzymatic paper.

Detection of Malathion in Contaminated Water, Plant, and Apple Samples

Water, soil, and apple samples were selected as typical contaminated matrices. 50 mM malathion and 2 mM Ellman's reagent were dissolved in the water, and sprayed on the surfaces of the plant leaves and the apples, respectively. Samples without malathion were used as controls. PF127–PAA–*Po*OPH$_{M9}$ papers were cut into strips and immersed in the water samples, or used to wipe the surfaces of the plant leaves and apples to detect malathion residues.

Results and Discussion

Preparation of PAA–*Po*OPH$_{M9}$ and PF127–PAA–*Po*OPH$_{M9}$ Papers

First, we improved the method developed by Riccardi et al. to physically trap enzyme–polymer conjugates within paper voids by interlocking with cellulose fibers. In this method, PAA, a negatively charged polymer with multiple carboxyl side groups, was cross-linked to the surface lysine residues of enzymes with the water-soluble carbodiimide EDC. In the original method, a neutral phosphate buffer (pH 7.0) was used for the cross-linking reaction. Considering that an alkaline solution can deprotonate the carboxylate groups of PAA and that *Po*OPH$_{M9}$ prefers a higher pH, we tested using a Tris-HCl buffer (pH 9.0) and a phosphate buffer (pH 7.0) to perform the reaction under the same conditions. Enzyme loading as a function of increasing PAA concentration (0, 20, 40, 60, 80, or 100 mg/mL) was examined with a fixed *Po*OPH$_{M9}$ concentration (10 mg/mL). With the pH 9.0 buffer, when the ratio of *Po*OPH$_{M9}$ to PAA was increased to 1:6, the enzyme loading of the filter paper increased to 97.4% (Fig. 1a). As the ratio of PAA continued to increase, the enzyme loading showed no further changes, indicating that this PAA concentration could immobilize almost all *Po*OPH$_{M9}$ on the filter paper. Notably, the enzyme loadings for all *Po*OPH$_{M9}$ to PAA ratios in the pH 9.0 buffer were all higher than those in the pH 7.0 buffer (average of 72%), which indicated that the alkaline solution favored the cross-linking reaction. Next, we measured the apparent activity of the enzyme immobilized on the paper in pH 7.0 and 9.0 buffers. In both buffers, the highest activity was found at a *Po*OPH$_{M9}$ to PAA ratio of 1:6, and again the immobilized enzyme in pH 9.0 buffer showed better activity (0.4 U/mg) than that in the pH 7.0 buffer (Fig. 1b). However, an excess of PAA did not improve the activity further because it blocked the surface of *Po*OPH$_{M9}$ and affected substrate binding of the enzyme. Considering both the enzyme loading and the apparent activity, a *Po*OPH$_{M9}$ to PAA ratio of 1:6 and Tris-HCl (pH

9.0) buffer were selected for subsequent experiments. The preparation of PF127–PAA–*Po*OPH$_{M9}$ papers was straightforward as *Po*OPH$_{M9}$ and PF127 were added directly to the activated PAA solution. Upon mixing, the reaction between *Po*OPH$_{M9}$ and PAA occurred as well as the conjugation of *Po*OPH$_{M9}$ with PF127. The reaction solution was immediately transferred to filter papers for immobilization.

Successful covalent attachment of *Po*OPH$_{M9}$ to PAA and an increase in the molecular weight were confirmed by SDS-PAGE (Fig. 1c). As a control, a set amount of purified *Po*OPH$_{M9}$ was analyzed and showed a clear band at 33 kDa. We used the same amount of enzyme for cross-linking. After the reaction, the enzyme–polymer conjugates were collected and subjected to SDS-PAGE. A much weaker band at 33 kDa was observed for the free, unreacted enzyme than in the control, and a broad and high molecular weight band appeared for PAA–*Po*OPH$_{M9}$. The broadness of the band could be attributed to the different number of enzymes attached to PAA and the wide PAA molecular weight range. To demonstrate the formation of PF127–PAA–*Po*OPH$_{M9}$, we performed the SDS-PAGE of PF127-PAA-*Po*OPH$_{M9}$ (Fig. 1d). Compared with the free *Po*OPH$_{M9}$ at 33 kDa, a weaker band at the same position was also observed for PF127-PAA-*Po*OPH$_{M9}$, which corresponded to the unreacted enzyme and similar to the observation in the PAA-*Po*OPH$_{M9}$ sample. In the PAA-*Po*OPH$_{M9}$ SDS-PAGE, a broad dispersive band corresponding to PAA-*Po*OPH$_{M9}$ was found; however,

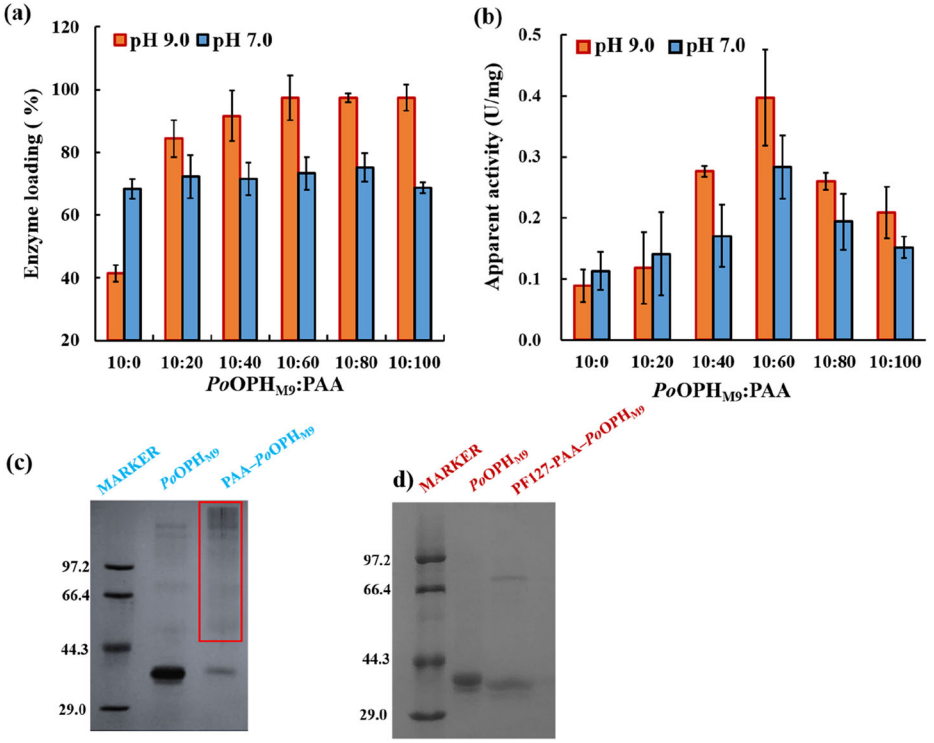

Fig. 1 Preparation of the PAA-*Po*OPH$_{M9}$ and PF127-PAA-*Po*OPH$_{M9}$ papers. Enzyme loading (**a**) and apparent activity (**b**) of PAA-*Po*OPH$_{M9}$ prepared in pH 7.0 and 9.0 buffer were measured, respectively. The total protein content (P_t) and the protein content in the washing water (P_w) were determined by the Coomassie brilliant blue method. The enzyme loading (%) of the paper-based biosensor was calculated according to Eq. 1. SDS-PAGE of the PAA-*Po*OPH$_{M9}$ (**c**) and the PF127-PAA-*Po*OPH$_{M9}$ (**d**) were performed to confirm the formation of the polymer-enzyme composite

in the PF127-PAA-*Po*OPH$_{M9}$ SDS-PAGE, a clear and relatively narrower band at ~70 kDa was observed for PF127-PAA-*Po*OPH$_{M9}$, which indicated that the interaction between the enzyme and PF127 influenced the covalent binding of the enzyme with PAA. This resulted in the formation of polymer-enzyme conjugates with narrow molecular weight dispersion, but the mechanism behind this result is still unclear now.

Malathion Detection by the PAA–*Po*OPH$_{M9}$ Paper

After optimization, the PAA–*Po*OPH$_{M9}$ paper was used to detect malathion. The enzyme kinetics were monitored by observing color changes over 60 min (Fig. 2a). The paper color clearly changed from white to dark yellow after addition of malathion. The kinetic profile of PAA–*Po*OPH$_{M9}$ was then measured by varying the malathion concentration (0.1–50 mM) and plotting the color intensity against time (Fig. 2b). Notably, the color intensities of all samples increased for the first 10 min and plateaued gradually after 20 min. The color intensity was higher for samples containing higher concentrations of malathion, which correlated well with earlier observations (Fig. 2a). From 30 to 60 min, the color faded and became paler in the center of paper (Fig. 2a). Therefore, 20 min was selected as the best time for discrimination among samples, and the color intensities at 20 min were measured and plotted against the concentration of malathion (Fig. 2c). The color intensities were linear between 0.1 and 1.0 mM, and plateaued when the concentration increased above 20 mM. Therefore, the detection range was 0.1 to 20 mM. Although this process took only 20 min, there was room for improvement. The initial rates of the reactions with the PAA–*Po*OPH$_{M9}$ papers were measured using the initial slopes of the curves (Fig. 2b) and fitted to the Michaelis–Menten model (Fig. 2d). The PAA-*Po*OPH$_{M9}$ paper had an apparent V_{max} of 7.1 ± 0.9 min^{-1} and K_m of 8.7 ± 3.2 mM.

Rapid Malathion Detection by the PF127–PAA–*Po*OPH$_{M9}$ Papers

We demonstrated previously that PF127 could stabilize and improve the activity of *Po*OPH$_{M9}$ during enzyme immobilization [29]. Inspired by this result, we hypothesized that PF127 could also improve the performance of malathion test papers. Consequently, we modified papers with PF127 during the cross-linking reaction. Different molar ratios of enzyme to PF127 (1:1, 1:2, 1:5, and 1:8) were used to prepare PF127–PAA–*Po*OPH$_{M9}$ papers. The color changes with the papers prepared with ratios of 1:1 and 1:8 are shown in Fig. 3a and b. The color of the PF127–PAA–*Po*OPH$_{M9}$ changed immediately after it came into contact with malathion and remained steady after 0.5 min, which was much faster than the detection with PAA–*Po*OPH$_{M9}$ (Fig. 3c and d). As the concentration of malathion increased (50–200 mM), the color intensity also increased, and 5 min was the best time to discriminate among samples with different malathion concentrations. PF127–PAA–*Po*OPH$_{M9}$ papers prepared with different enzyme to PF127 molar ratios showed similar dynamic behavior for the color intensity in a malathion concentration range of 0.1–50 mM (Fig. 3e), and plateaued when the malathion concentration was above 50 mM. The PF127–PAA–*Po*OPH$_{M9}$ paper prepared with an enzyme to PF127 molar ratio of 1:8 showed slightly better detection performance than the other papers, so it was used in subsequent experiments. Compared with the PAA-*Po*OPH$_{M9}$ paper, the apparent V_{max} of the PF127-PAA-*Po*OPH$_{M9}$ paper was higher at 15.3 ± 1.8 min^{-1}, and the K_m was nearly the same (7.3 ± 3.3 mM) (Fig. 3f). Distinguished from the kinetic plot in Fig. 2d, the reaction catalyzed by PF127-PAA-*Po*OPH$_{M9}$ was so rapid that the color changed immediately (especially for the high substrate concentration). Therefore, the initial reaction rates were flatted at

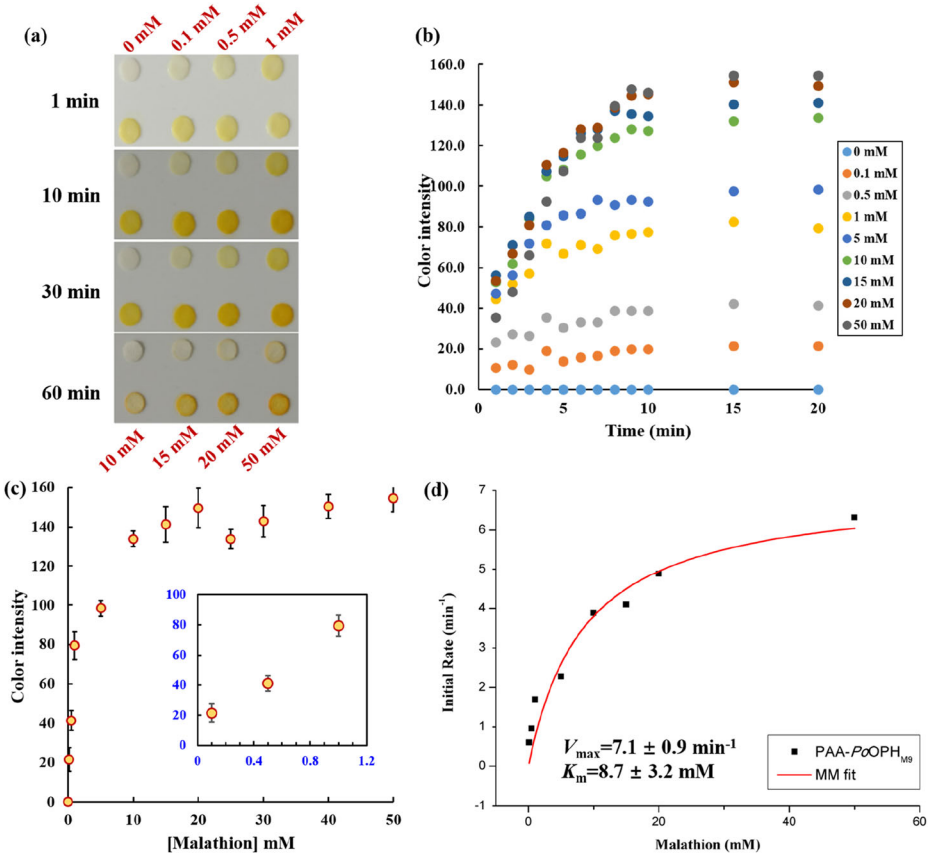

Fig. 2 Detection of malathion using the PAA-*Po*OPH$_{M9}$ paper. (**a**) Monitoring color change over time with respect to (malathion). Images were taken every 1 min for the first 10 min, then every 5 min up to 60 min. **b** Enzymatic kinetic traces down from the color intensities before 20 min in panel **a**. **c** Color intensities at 20 min with respect to (malathion). **d** The apparent kinetic parameters were determined by fitting the reaction rates at different substrate concentrations to the Michaelis-Menten equation

high substrate concentrations quickly and the measured values may be underestimated, which made it difficult to draw accurate kinetic curves in these conditions.

According to studies reported by other groups [30, 31], the activity and stability of free OPHs can be improved by PF127 through the interaction between the hydrophobic poly(propylene oxide) (PPO) block of PF127 and the hydrophobic amino acids of enzyme surface. This was also demonstrated in our previous studies that the activity of *Po*OPH$_{M9}$ was enhanced by PF127 during the formation of cross-linked enzyme aggregates [29]. Here, we found the enzyme loading efficiency was 75% ± 4% for PF127–PAA–*Po*OPH$_{M9}$ and 93.5% ± 3.8% for PAA–*Po*OPH$_{M9}$ (Table S1), which indicated the protein loading of PF127–PAA–*Po*OPH$_{M9}$ was lower than that of PAA–*Po*OPH$_{M9}$. The addition of PF127 may reduce the cross-linking of PAA with the enzyme and lower the interlocking of enzyme within the cellulose fibers in the paper. The total improved V_{max} and the reduced protein content indicated the intrinsic catalysis (k_{cat}) was improved, which agrees well with the previous reports. In Kim et al. study [31], they demonstrated that other PPO-containing block polymers can also improve the activity and stability of OPHs. However, this is not general for enzymes other than OPHs.

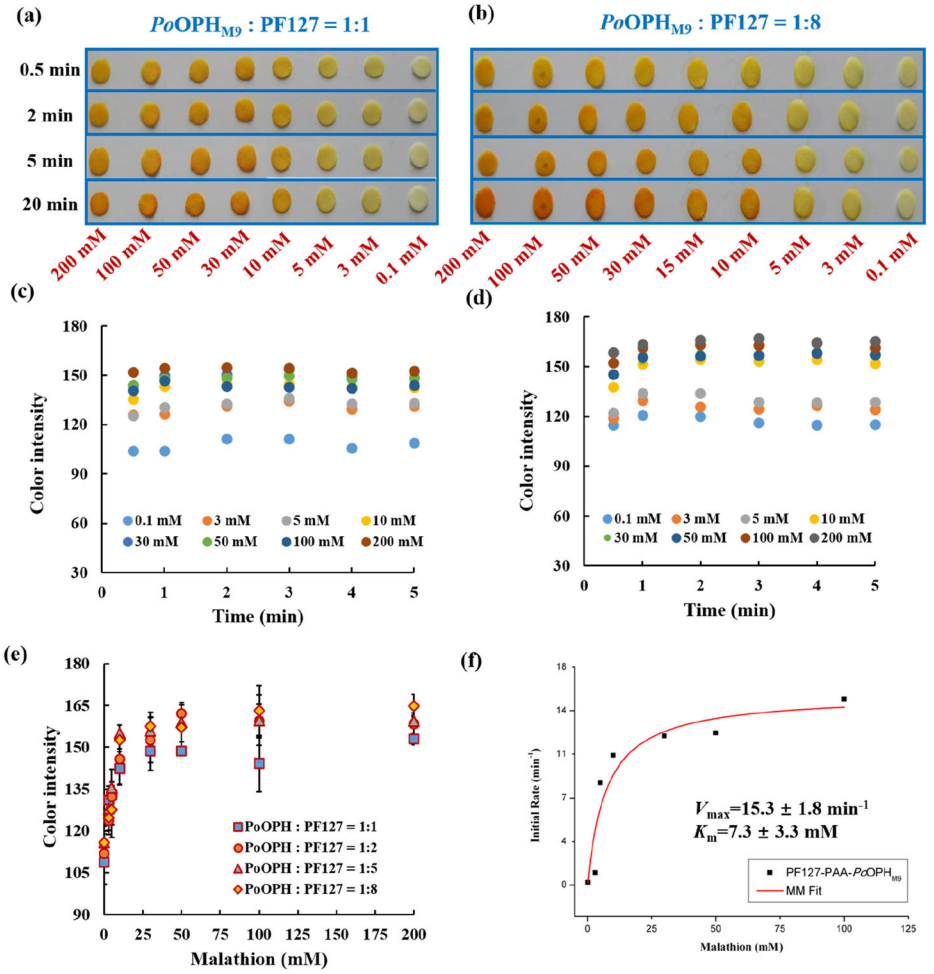

Fig. 3 Rapid detection of malathion using the PF127-PAA-*Po*OPH$_{M9}$ paper. **a**, **b** Monitoring color change over time with respect to the molar ratio of *Po*OPH$_{M9}$ to PF127 (1:1, **a**; 1:8, **b**). **c**, **d** Enzymatic kinetic traces down from the color intensities within 5 min in panel **a** and **b**. **e** Color intensities at 5 min with respect to (malathion) and the molar ratio of *Po*OPH$_{M9}$ to PF127. **f** The apparent kinetic parameters were determined by fitting the reaction rates at different substrate concentrations to the Michaelis-Menten equation

Previously, we tried to improve the activity of enzymes such as ketoreductases by the addition of PF127 in the enzyme solution, but did not find the formation of polymer-enzyme conjugates nor the improvement in the OPH case (data not shown). To date, a detailed mechanism for the improvement of OPHs by PF127 has not been elucidated. In this study, the novelty is that PF127 can also improve the activity of OPH when they are covalently bonded with PAA during immobilization, which enhanced the whole performance of paper-based biosensors. Considering various enzymes can be modified by direct conjugation or covalent binding with polymers [32], we suggest that many biocompatible polymers should be investigated whether they can improve the activity and stability of enzymes used in biosensors because these enzymes are working as the key signal-transduction component in non-natural environment and a slight improvement in catalytic properties will enhance the whole performance of biosensors significantly.

Specificity and Storage of the Paper-Based Biosensors

The specificity of the paper-based biosensor is important for practical application as it determines the accuracy of this method. To understand whether the detection of malathion is influenced by other pesticides, we purchased 4 other pesticides (methyl parathion, dimethoate, carbaryl, and DDT) and performed detection experiments towards these 4 pesticides and malathion as well as the blank controls. The blank control was performed by adding the PBS buffer without any pesticides. As shown in Fig S2, only the paper contaminated by 5 mM malathion showed the color change from white to yellow, and other papers showed no changes compared with the negative control. This result demonstrated that this paper biosensor has a high specificity towards malathion.

To test the storage stability, the PF127–PAA–*Po*OPH$_{M9}$ papers were prepared and stored in an open-air environment as well as in a vacuum bag. For comparison, all samples were stored at room temperature, and their capability of detecting 5 and 50 mM malathion was tested after different days and compared with the newly prepared sample (day 0, Fig S2). The samples stored in air quickly lost the capability of detecting 5 mM malathion after 1 day; however, the samples stored in vacuum can detect it after 3 days and lost its activity after 5 days. For the detection of 50 mM malathion, the two samples did not show such big difference and both can detect it after 3 days, and in day 5 they can still detect malathion although the color intensity decreased a lot. In conclusion, the sensitivity of the paper biosensor was influenced by oxidation when stored in air at room temperature, and preservation in vacuum can improve its stability for storage. Considering these tests were performed at room temperature, the lower storage temperature, such as 4 °C, can keep its activity for a longer time.

Detection of Malathion in Contaminated Water, Soil, and Fruit Samples

Next, we evaluated the capacity of the PF127–PAA–*Po*OPH$_{M9}$ paper for rapid, on-site detection of malathion residues in the environment. The PF127–PAA–*Po*OPH$_{M9}$ papers showed obvious color changes after contact with the contaminated samples for 5 min, and these changes could be observed by the naked eye (Fig. 4). By contrast, PF127–PAA–*Po*OPH$_{M9}$ papers used on samples without malathion contamination did not show color changes. Photographs were taken with a smartphone, and the images could be stored, transmitted, and analyzed by software for quantification. If an application for image analysis was installed on the smartphone, detection of malathion in the field could be completed within a couple of minutes. Because the PF127–PAA–*Po*OPH$_{M9}$ papers are cheap and easy to fabricate, this method is inexpensive and physically flexible for detecting malathion on different contaminated surfaces by wiping.

Conclusions

In this work, we developed an interlocking method for immobilization of polymer–enzyme conjugates in filter papers, and applied it to fabricate cheap papers for efficient malathion detection. A pH of 9.0 was favorable for the retention of the activity of immobilized *Po*OPH$_{M9}$. The PAA–*Po*OPH$_{M9}$ papers could detect malathion at concentrations between 0.1 and 20 mM. Addition of PF127 reduced the detection time for the PF127–PAA–*Po*OPH$_{M9}$ paper to 5 min and increased the V_{max} two-fold. The PF127–PAA–*Po*OPH$_{M9}$ paper is

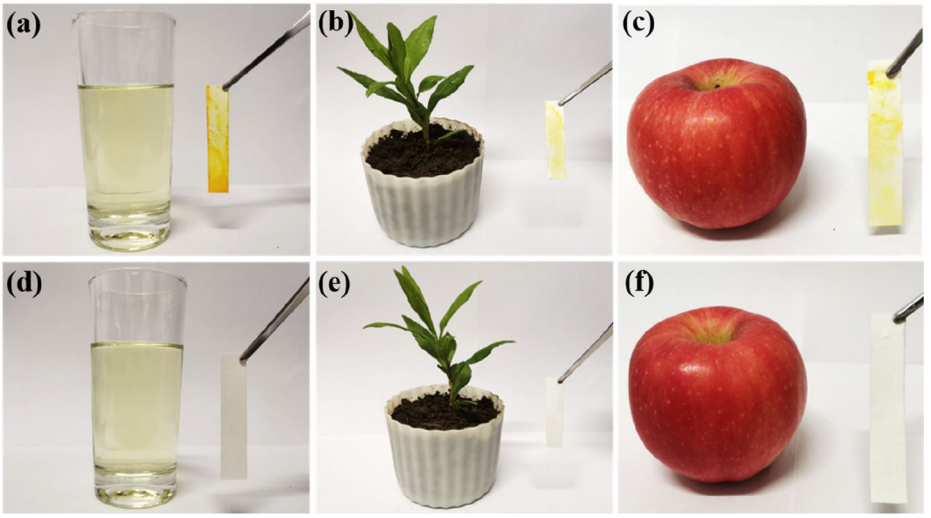

Fig. 4 On-site analysis of malathion in different samples. Digital photos of malathion detection in water (**a**), on plant leaves (**b**), and apple surfaces (**c**). Samples without malathion contamination were detected as the blank controls (**d**, **e**, **f**)

inexpensive and physically flexible that can facilitate its use for malathion detection in samples with different forms within a couple of minutes. This is a novel approach for real-time and on-site acquisition of organophosphorus residue information, and provides new insight into the design of next generation paper-based biosensors.

Supplementary Information The online version contains supplementary material available at https://doi.org/10.1007/s12010-021-03531-x.

Author Contribution X.-Y. Zhang and Y.-P. Bai designed and instructed the experiments; J.-H. Li, X.-L. Deng, and Y.-L. Zhao performed the research experiments; J.-H. Li, X.-L. Deng, Y.-L. Zhao, X.-Y. Zhang, and Y.-P. Bai analyzed the data; J.-H. Li, X.-Y. Zhang, and Y.-P. Bai wrote the manuscript. All authors read and approved the final manuscript.

Funding This work was financially sponsored by the National Key Research and Development Program of China (2016YFA0204300), the Natural Science Foundation of Shanghai (18ZR1409900), and the Key Project of the Shanghai Science and Technology Committee (18DZ1112703).

Data Availability Not applicable.

Declarations

Ethical Approval Not applicable

Consent to Participate Not applicable.

Consent to Publish Not applicable

Competing Interests The authors declare no competing interests.

References

1. Giudice, I., Coppolecchia, R., Merone, L., Porzio, E., Carusone, T., Mandrich, L., Worek, F., & Manco, G. (2015). An efficient thermostable organophosphate hydrolase and its application in pesticide decontamination. *Biotechnology and Bioengineering, 113*, 724–734.
2. EPA, Malathion. https://www.epa.gov/mosquitocontrol/malathion (accessed September 13, 2020).
3. Mostafalou, S., & Abdollahi, M. (2017). Pesticides: an update of human exposure and toxicity. *Archives of Toxicology, 91*(2), 549–599.
4. Cycon, M., Mrozik, A., & Piotrowska-Seget, Z. (2017). Bioaugmentation as a strategy for the remediation of pesticide-polluted soil: a review. *Chemosphere, 172*, 52–71.
5. Hernandez, A. F., Gil, F., & Lacasana, M. (2017). Toxicological interactions of pesticide mixtures: an update. *Archives of Toxicology, 91*(10), 3211–3223.
6. Sapahin, H. A., Makahleh, A., & Saad, B. (2019). Determination of organophosphorus pesticide residues in vegetables using solid phase micro-extraction coupled with gas chromatography–flame photometric detector. *Arabian Journal of Chemistry, 12*(8), 1934–1944.
7. Harshit, D., Kothari, C., & Nrupesh, P. (2017). Organophosphorus pesticides determination by novel HPLC and spectrophotometric method. *Food Chemistry, 230*, 448–453.
8. Chen, Q., & Fung, Y. (2010). Capillary electrophoresis with immobilized quantum dot fluorescence detection for rapid determination of organophosphorus pesticides in vegetables. *Electrophoresis, 31*(18), 3107–3114.
9. Mishra, R. K., Istamboulie, G., Bhand, S., & Marty, J.-L. (2012). Detoxification of organophosphate residues using phosphotriesterase and their evaluation using flow based biosensor. *Analytica Chimica Acta, 745*, 64–69.
10. Arduini, F., Cinti, S., Caratelli, V., Amendola, L., Palleschi, G., & Moscone, D. (2019). Origami multiple paper-based electrochemical biosensors for pesticide detection. *Biosensors and Bioelectronics, 126*, 346–354.
11. Qiu, Z., Shu, J., & Tang, D. (2017). Bioresponsive release system for visual fluorescence detection of carcinoembryonic antigen from mesoporous silica nanocontainers mediated optical color on quantum dot-enzyme-impregnated paper. *Analytical Chemistry, 89*(9), 5152–5160.
12. Boehle, K. E., Carrell, C. S., Caraway, J., & Henry, C. S. (2018). Paper-based enzyme competition assay for detecting falsified β-lactam antibiotics. *ACS Sensors, 3*(7), 1299–1307.
13. Böhm, A., Trosien, S., Avrutina, O., Kolmar, H., & Biesalski, M. (2018). Covalent attachment of enzymes to paper fibers for paper-based analytical devices. *Frontiers in Chemistry, 6*, 214.
14. Hossain, S. M., Luckham, R. E., McFadden, M. J., & Brennan, J. D. (2009). Reagentless bidirectional lateral flow bioactive paper sensors for detection of pesticides in beverage and food samples. *Analytical Chemistry, 81*(21), 9055–9064.
15. Hossain, S. M., Luckham, R. E., Smith, A. M., Lebert, J. M., Davies, L. M., Pelton, R. H., et al. (2009). Development of a bioactive paper sensor for detection of neurotoxins using piezoelectric inkjet printing of sol-gel-derived bioinks. *Analytical Chemistry, 81*(13), 5474–5483.
16. Credou, J., & Berthelot, T. (2014). Cellulose: from biocompatible to bioactive material. *Journal of Material Chemistry B, 2*(30), 4767–4788.
17. Sulaiman, S., Mokhtar, M. N., Naim, M. N., Baharuddin, A. S., & Sulaiman, A. (2015). A review: potential usage of cellulose nanofibers (CNF) for enzyme immobilization via covalent interactions. *Applied Biochemistry and Biotechnology, 175*(4), 1817–1842.
18. Xing, Q., Eadula, S. R., & Lvov, Y. M. (2007). Cellulose fiber−enzyme composites fabricated through layer-by-layer nanoassembly. *Biomacromolecules, 8*(6), 1987–1991.
19. Kannan, B., Jahanshahi-Anbuhi, S., Pelton, R. H., Li, Y., Filipe, C. D., & Brennan, J. D. (2015). Printed paper sensors for serum lactate dehydrogenase using pullulan-based inks to immobilize reagents. *Analytical Chemistry, 87*(18), 9288–9293.
20. Nuchtavorn, N., Leanpolchareanchai, J., Suntornsuk, L., & Macka, M. (2020). Paper-based sol-gel thin films immobilized cytochrome P450 for enzyme activity measurement. *Analytica Chimica Acta, 1098*, 86–93.
21. Zhang, L. T., Cao, X. D., Wang, L., Zhao, X. Y., Zhang, S. P., & Wang, P. (2015). Printed microwells with highly stable thin-film enzyme coatings for point-of-care multiplex bioassay of blood samples. *Analyst, 140*(12), 4105–4413.
22. Zhang, Y. F., Lyu, F. J., Ge, J., & Liu, Z. (2014). Ink-jet printing an optimal multi-enzyme system. *Chemical Communications, 50*(85), 12919–12922.
23. Riccardi, C., Mistri, D., Hart, O., Anuganti, M., Lin, Y., Kasi, R., & Kumar, C. (2016). Covalent interlocking of glucose oxidase and peroxidase in the voids of paper: enzyme-polymer "spider webs". *Chemical Communication, 52*(12), 2593–2596.

24. Luo, X. G., Xia, J., Jiang, X. Y., Yang, M. R., & Liu, S. L. (2019). Cellulose-based strips designed based on a sensitive enzyme colorimetric assay for the low concentration of glucose detection. *Analytical Chemistry, 91*(24), 15461–15468.
25. Park, C. Y., Kim, H. R., Kim, S. K., Jeong, I. K., Pyun, J. C., & Park, S. S. (2019). Three-dimensional paper-based microfluidic analytical devices integrated with a plasma separation membrane for the detection of biomarkers in whole blood. *ACS Applied Materials & Interfaces, 11*(40), 36428–36434.
26. Liu, M. M., Lian, X., Liu, H., Guo, Z. Z., Huang, H. H., Lei, Y., Peng, H. P., Chen, W., Lin, X. H., Liu, A. L., & Xia, X. H. (2019). A colorimetric assay for sensitive detection of hydrogen peroxide and glucose in microfluidic paper-based analytical devices integrated with starch-iodide-gelatin system. *Talanta, 200*, 511–517.
27. Luo, X. J., Zhao, J., Li, C. X., Bai, Y. P., Reetz, M. T., Yu, H. L., & Xu, J. H. (2016). Combinatorial evolution of phosphotriesterase toward a robust malathion degrader by hierarchical iteration mutagenesis. *Biotechnology & Bioengineering, 113*(11), 2350–2357.
28. Bai, Y. P., Luo, X. J., Zhao, Y. L., Li, C. X., Xu, D. S., & Xu, J. H. (2017). Efficient degradation of malathion in the presence of detergents using an engineered organophosphorus hydrolase highly expressed by *Pichia pastoris* without methanol induction. *Journal of Agricultural and Food Chemistry, 65*(41), 9094–9100.
29. Cheng, H., Zhao, Y. L., Luo, X. J., Xu, D. S., Cao, X., Xu, J. H., Dai, Q., Zhang, X. Y., Ge, J., & Bai, Y. P. (2018). Cross-linked enzyme-polymer conjugates with excellent stability and detergent-enhanced activity for effcient organophosphate degradation. *Bioresources and Bioprocessing, 5*(1), 49.
30. Suthiwangcharoen, N., & Nagarajan, R. (2014). Enhancing enzyme stability by construction of polymer–enzyme conjugate micelles for decontamination of organophosphate agents. *Biomacromolecules, 15*(4), 1142–1152.
31. Kim, M., Gkikas, M., Huang, A., Kang, J. W., Suthiwangcharoen, N., Nagarajan, R., & Olsen, B. D. (2014). Enhanced activity and stability of organophosphorus hydrolase via interaction with an amphiphilic polymer. *Chemical Communication, 50*(40), 5345–5348.
32. Wu, X. L., Ge, J., Zhu, J. Y., Zhang, Y. F., Yong, Y., & Liu, Z. (2015). A general method for synthesizing enzyme-polymer conjugates in reverse emulsions using Pluronic as a reactive surfactant. *Chemical Communication, 51*(47), 9674–9677.